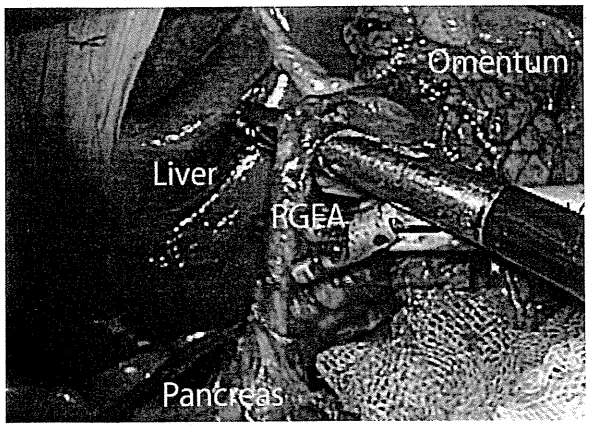

Figure 4 Skeletonization around RGEA in case 2. RGEA: right gastroepiploic artery.

RGEA thickness was almost normal, and skeletonization was easily performed using the USAD as in the previous case (Figure 4). The fine vessels distributed from the RGEA over the pylorus and bulbs were also easily dissected using the USAD. Coronary CT angiography showed poor RGEA graft patency. However, we opted for an RGEA-preserving surgery because no metastatic lymph nodes in the no. 6 area could be identified by either CT and on intraoperative observation. Prophylactic dissection of the no. 6 lymph node was possible without injury to the RGEA or intraoperative arrhythmias. Additional lymph node dissection was performed in accordance with typical LDG procedures. Continuous nicorandil injection was used during the surgery to prevent angina. The operative time was 295 min, and blood loss was 61 mL. The patient was discharged on postoperative day 10 without any complications.

Currently, the patient is alive without any signs of recurrence or heart failure. According to pathologic findings, the resected specimen was 7.0 × 7.0 cm in diameter, tub2, T3, n3b, ly2, v2, and stage IIIB. There was no lymph node metastasis along the RGEA.

Discussion

CABG for ischemic heart disease often uses the RGEA, in addition to the internal thoracic artery, as a reliable conduit with long-term patency. However, problems may be encountered if patients must later undergo gastrectomy for gastric cancer because the RGEA should be harvested along with the lymph nodes (1–6). In such cases, the following two possibilities for lymph node dissection exist: one involves preserving the RGEA and the other involves dissection including the RGEA. Kubo *et al.* summarized gastrectomy cases with grafted RGEA and reported 16 preserving cases and 10 resection cases (5). Mita *et al.* reported two preserving cases and six resection cases in their experiences (6). These reports did not distinguish between the criteria used to decide whether RGEA resection and RGEA preserving was most appropriate, and there appears to be no other information on choosing between these procedures. However, in cases in which lymph node metastasis is negative, we believe that the grafted RGEA should be preserved by skeletonized no. 6 lymph node dissection. This procedure is feasible in the same way as lymph node dissection with the common hepatic artery or splenic artery. Regardless of the procedure used, specific preparations corresponding to each method are required. In cases in which resection of the patent RGEA graft is planned, percutaneous coronary intervention or a second bypass surgery using another vessel is required prior to gastrectomy (4,6). In cases of early gastric cancer or advanced gastric cancer without obvious lymph node metastasis, the RGEA graft is usually preserved and careful lymph node dissection and anti-spasm agents are required (1–3,5). Recent retrospective studies of laparoscopic gastrectomy for advanced gastric cancer showed the good long-term prognosis for patients, but there has been no prospective randomized trial to date (8–10). Therefore, laparoscopic surgery is not currently accepted as a standard procedure for advanced gastric cancer.

We began performing laparoscopic gastrectomy with D2 lymph node dissection in 2004, and over the years, the indication of laparoscopic gastrectomy gradually extended to advanced gastric cancer (11). Although laparoscopic gastrectomy for advanced gastric cancer remains controversial, we do perform it for advanced gastric cancer without bulky lymph node metastasis. Patients must provide approval for the procedure. In case 2 in this report, we performed LDG for advanced gastric cancer at the patient's request.

Intraoperative injury to the RGEA graft from a laparotomy procedure or from the use of a wound retractor is a distinct possibility. It is also possible to inflict injury during skeletonizing of the RGEA or no. 6 lymph node dissection. The grafted RGEA with adhesions usually lies under the area between the midline of the upper abdomen and the heart; therefore, in open surgery, meticulous laparotomy and vigilant retractor management are required to avoid direct injury to the RGEA. In contrast, laparoscopic surgery can avoid risks of injury to the RGEA from either a laparotomy or a retractor. Furthermore, port locations used during laparoscopic surgery are placed a reasonable distance from the grafted RGEA and the adhesions resulting from bypass surgery. Identification of the grafted RGEA is possible using

typical laparoscopic settings that offer a good view of the surgical field. Despite this, there are some disadvantages associated with laparoscopic surgery; for example, manipulation is technically more difficult than in open surgery. Therefore, in the laparoscopic approach, skeletonizing of the RGEA and no. 6 lymph node dissection while preserving the RGEA require more discernment than in open surgery. However, based on our experience, the possibility of injury to the RGEA is considerably low, particularly in cases with patent grafts because they tend to become thicker.

Additionally, for patients with the RGEA graft and no. 6 lymph node dissection, another technical problem with laparoscopic-assisted gastrectomy (LAG) is that typically an assistant grasps and hoists the pedicle of the RGEA to access the dissection area of the no. 6 lymph node. However, this dissection must be performed without grasping the RGEA. In these two cases, we performed no. 6 lymph node dissection by grasping the great curvature site and nearby fat tissue separating the grafted RGEA from the stomach instead of grasping the pedicle of the RGEA.

Intraoperative provisions for spasms include drug therapy and careful surgical manipulation. Continuous nicorandil or nitroglycerine injection and sprinkling papaverine hydrochloride around the RGEA have been reported as treatment for spasms (3). Careful RGEA skeletonization and no. 6 lymph node dissection are also required to avoid spasms. In addition, the heat effect of energy devices should be considered. USAD, which radiates less heat than electrocautery, is often used during LAG, which can perhaps be considered an additional merit of this method. Naturally, it is important that the active blade of a USAD must not turn on the graft side to avoid thermal injury. Safety assessments of artery skeletonization using USAD were reported in some cardiovascular surgery fields (12,13). In these reports, the USAD method was faster, easier and safer than using electrocautery and scissors, caused less bleeding, and obtained a spasm-free conduit condition (12,13). We believe that similar results could be obtained in laparoscopic surgery, and in our experience, the risk of intraoperative arterial injury is relatively low. However, this operation should be performed at a hospital in which cardiologists and cardiovascular surgeons can be on standby in case of accidental injury to the RGEA during surgery.

In conclusion, we safely performed LAG, preserving the RGEA graft in patients who had previously undergone CABG surgery. We consider LAG to be less invasive than open gastrectomy and to have a lower risk of injury to the RGEA graft. We believe that LAG performed by a qualified and experienced surgeon is a reasonable procedure for patients who have previously undergone CABG using the RGEA and who lack obvious no. 6 lymph node metastasis.

Acknowledgment

The authors have no conflicts of interest or financial ties to disclose.

References

1. Hashiguchi N, Kubota T, Otani Y *et al.* Surgery for advanced gastric cancer after coronary artery bypass grafting using the right gastroepiploic artery: Report of a case. *Surg Today* 2004; **34**: 456–458.
2. Shimizu J, Hirano Y, Kinoshita S *et al.* Gastric cancer occurred after coronary artery bypass grafting using the right gastroepiploic artery. *Ann Thorac Cardiovasc Surg* 2004; **10**: 255–258.
3. Konishi Y, Suzuki K, Wada H *et al.* How do we manage the gastrectomy for gastric cancer after coronary artery bypass grafting using the right gastroepiploic artery? Report of two cases and a review of the literature. *World J Surg Oncol* 2007; **5**: 54.
4. Shinkura N, Mitsuyoshi A, Obama K *et al.* Distal gastrectomy with reconstruction of the right gastroepiploic artery for gastric cancer after coronary artery bypass grafting: Report of a case. *Surg Today* 2008; **38**: 548–551.
5. Kubo N, Oki E, Ohgaki K *et al.* Surgical resection following combination chemotherapy with oral S-1 and biweekly docetaxel in a patient with advanced gastric cancer and a prior coronary artery bypass graft with the right gastroepiploic artery: Report of a case. *Surg Today* 2011; **41**: 1531–1537.
6. Mita K, Ito H, Fukumoto M *et al.* An adequate perioperative management and strategy for gastric cancer after coronary artery bypass using the right gastroepiploic artery. *Surg Today* 2012; **43**: 284–288.
7. Japanese Gastric Cancer Association. Japanese classification of gastric carcinoma: 3rd English edition. *Gastric Cancer* 2011; **14**: 101–112.
8. Gordon AC, Kojima K, Inokuchi M *et al.* Long-term comparison of laparoscopy-assisted distal gastrectomy and open distal gastrectomy in advanced gastric cancer. *Surg Endosc* 2013; **27**: 462–470.
9. Uyama I, Suda K, Satoh S. Laparoscopic surgery for advanced gastric cancer: Current status and future perspectives. *J Gastric Cancer* 2013; **13**: 19–25.
10. Fang C, Hua J, Li J *et al.* Comparison of long-term results between laparoscopy-assisted gastrectomy and open gastrectomy with D2 lymphadenectomy for advanced gastric cancer. *Am J Surg* 2014. doi: 10.1016/j.amjsurg.2013.09.028

11. Kawamura H, Homma S, Yokota R. Inspection of safety and accuracy of D2 lymph node dissection in laparoscopy-assisted distal gastrectomy. *World J Surg* 2008; **32**: 2366–2370.
12. Amano A, Takahashi A, Hirose H. Skeletonized radial artery grafting: Improved angiographic results. *Ann Thorac Surg* 2002; **73**: 1880–1887.
13. Asai T & Shigeki T. Skeletonization of right gastroepiploic artery using an ultrasonic scalpel. *Ann Thorac Surg* 2002; **74**: 1715–1717.

THE JOURNAL OF BIOLOGICAL CHEMISTRY VOL. 289, NO. 38, pp. 26607–26617, September 19, 2014

Diacylglycerol Kinase δ Phosphorylates Phosphatidylcholine-specific Phospholipase C-dependent, Palmitic Acid-containing Diacylglycerol Species in Response to High Glucose Levels*

Received for publication, June 20, 2014, and in revised form, August 8, 2014 Published, JBC Papers in Press, August 11, 2014, DOI 10.1074/jbc.M114.590950

Hiromichi Sakai[‡], **Sayaka Kado**[§], **Akinobu Taketomi**[¶], **and Fumio Sakane**[‡1]

From the [‡]*Department of Chemistry, Graduate School of Science and* [§]*Center for Analytical Instrumentation, Chiba University, 1-33 Yayoi-cho, Inage-ku, Chiba 263-8522 and the* [¶]*Department of General Surgery, Graduate School of Medicine, Hokkaido University, North 15, West 7, Kita-ku, Sapporo 060-8638, Japan*

Background: Diacylglycerol (DG) kinase (DGK) δ is activated by acute high glucose stimulation.
Results: DGKδ high glucose-dependently phosphorylates 30:0-, 32:0-, and 34:0-DG and interacts with phosphatidylcholine-specific phospholipase C (PC-PLC).
Conclusion: DGKδ utilizes palmitic acid-containing DG species and metabolically connects with PC-PLC.
Significance: The newly identified PC-PLC/DGKδ pathway could play an important role in insulin signaling and glucose uptake.

Decreased expression of diacylglycerol (DG) kinase (DGK) δ in skeletal muscles is closely related to the pathogenesis of type 2 diabetes. To identify DG species that are phosphorylated by DGKδ in response to high glucose stimulation, we investigated high glucose-dependent changes in phosphatidic acid (PA) molecular species in mouse C2C12 myoblasts using a newly established liquid chromatography/MS method. We found that the suppression of DGKδ2 expression by DGKδ-specific siRNAs significantly inhibited glucose-dependent increases in 30:0-, 32:0-, and 34:0-PA and moderately attenuated 30:1-, 32:1-, and 34:1-PA. Moreover, overexpression of DGKδ2 also enhanced the production of these PA species. MS/MS analysis revealed that these PA species commonly contain palmitic acid (16:0). D609, an inhibitor of phosphatidylcholine-specific phospholipase C (PC-PLC), significantly inhibited the glucose-stimulated production of the palmitic acid-containing PA species. Moreover, PC-PLC was co-immunoprecipitated with DGKδ2. These results strongly suggest that DGKδ preferably metabolizes palmitic acid-containing DG species supplied from the PC-PLC pathway, but not arachidonic acid (20:4)-containing DG species derived from the phosphatidylinositol turnover, in response to high glucose levels.

Type 2 diabetes is expected to afflict over 300 million people worldwide by 2015 (1). The characteristic features of type 2 diabetes include insulin resistance, glucose intolerance, hyperglycemia, and often, hyperinsulinemia (2). Glucose-induced insulin resistance is associated with a temporal increase in the intracellular diacylglycerol (DG)[2] mass in skeletal muscle (3).

DG is metabolized, at least in part, by DG kinase (DGK), which phosphorylates DG to generate phosphatidic acid (PA) (4–8). To date, 10 mammalian DGK isozymes (α, β, γ, δ, η, κ, ϵ, ζ, ι, and θ) have been identified, and these isozymes are subdivided into five groups according to their structural features (6, 7). Type II DGKs consist of the δ, η, and κ isoforms (9, 10). Moreover, alternatively spliced forms of DGKδ (δ1 and δ2) (11) and η (η1 and η2) (12) have been found.

DGKδ is highly expressed in skeletal muscle (13), which is a major insulin-target organ for glucose disposal (14). Chibalin *et al.* (15) demonstrated that DGKδ regulates glucose uptake and that a decrease in DGKδ expression resulted in the aggravation of type 2 diabetes. Long term exposure (96 h) to high glucose medium decreased DGKδ protein levels in primary cultured skeletal muscle cells, and the transcription of DGKδ and the levels of DGKδ protein were also reduced in skeletal muscles from type 2 diabetes patients (15). Moreover, DGKδ haploinsufficient mice ($DGK\delta^{+/-}$) exhibited decreased total DGK activity, reduced DGKδ protein levels, and the accumulation of DG in skeletal muscle. The increase in the amount of DG caused the increase in the phosphorylation of protein kinase C (PKC) δ and a reduction in the expression of the insulin receptor and insulin receptor substrate-1 proteins involved in insulin signaling (15). Furthermore, Miele *et al.* (16) reported that acute high glucose exposure (within 5 min) increased DGKδ activity in skeletal muscle cells followed by a reduction of PKCα activity and transactivation of the insulin receptor signal.

* This work was supported in part by grants from the Ministry of Education, Culture, Sports, Science and Technology of Japan; the Japan Science and Technology Agency; the Naito Foundation; the Hamaguchi Foundation for the Advancement of Biochemistry; the Daiichi-Sankyo Foundation of Life Science; the Terumo Life Science Foundation; the Futaba Electronic Memorial Foundation; the Daiwa Securities Health Foundation; the Ono Medical Research Foundation; the Japan Foundation for Applied Enzymology; and the Food Science Institute Foundation.
[1] To whom correspondence should be addressed. Tel./Fax: 81-43-290-3695; E-mail: sakane@faculty.chiba-u.jp.

[2] The abbreviations used are: DG, diacylglycerol; DGK, DG kinase; D609, *O*-tricyclo[5.2.1.$0^{2,6}$]dec-9-yl dithiocarbonate; FIPI, 5-fluoro-2-indolyl deschlorohalopemide; ESI, electrospray ionization; PA, phosphatidic acid; PC, phosphatidylcholine; PC-PLC, PC-specific phospholipase C; PLD, phospholipase D; TOFA, 5-(tetradecyloxy)-2-furoic acid; PI, phosphatidylinositol; DMSO, dimethyl sulfoxide; AcGFP, GFP from *Aequorea coerulescens*.

Hence, these studies indicate that DG consumed by DGKδ in response to high glucose exposure is a key regulator of glucose uptake in skeletal muscle cells. DGKδ1 translocated from the cytoplasm to the plasma membrane in mouse myoblast C2C12 cells within 5 min of short term exposure to a high glucose concentration, whereas DGKδ2 was located in punctate vesicles irrespective of the glucose concentration (17).

Mammalian cells contain at least 50 structurally distinct molecular DG species because DG contains a variety of fatty acyl moieties at positions 1 and 2 (18). In general, DGs containing arachidonic acid (20:4), especially 18:0/20:4-DG (38:4-DG), in the phosphatidylinositol (PI) turnover are important molecules that serve as second messengers for PKC activation (18). Moreover, previous studies have demonstrated that DGKε preferably phosphorylates arachidonic acid-containing DGs derived from PI turnover (19, 20). Therefore, it is generally believed that all DGKs preferentially metabolize 38:4-DG for the regulation of signal transduction. However, the DG molecular species phosphorylated by DGKδ in response to glucose stimulation remain unknown.

In this study, we investigated the changes in the amounts of PA molecular species that are produced by DGK in glucose-stimulated C2C12 myoblasts using our previously developed liquid chromatography/electrospray ionization mass spectrometry (LC/ESI-MS) method (21) to identify the DG molecular species metabolized by DGKδ under short term high glucose conditions. Interestingly, the LC/ESI-MS analyses indicated that DGKδ preferably metabolizes limited DG molecular species, 30:0-, 30:1-, 32:0-, 32:1-, 34:0-, and 34:1-DG, commonly containing palmitic acid (16:0), but not DG species containing arachidonic acid in response to high glucose stimulation. Moreover, the 30:0-, 32:0-, and 34:0-DG species were suggested to be supplied by phospholipase C (PLC)-dependent phosphatidylcholine (PC) hydrolysis, indicating an unexpected linkage between PC-PLC and DGKδ.

EXPERIMENTAL PROCEDURES

Cell Culture—C2C12 mouse myoblasts were maintained on 100-mm dishes in DMEM (Wako Pure Chemicals) containing 10% FBS (Biological Industries-Invitrogen) at 37 °C in an atmosphere containing 5% CO_2. For differentiation to myotubes, confluent C2C12 myoblasts were cultured in differentiation medium (DMEM containing 0.1% FBS and 5 μg/ml insulin (Sigma-Aldrich)) for 4 days.

Establishment of a Stable Cell Line Overexpressing DGKδ—To establish C2C12 cells stably expressing human DGKδ2, the cells were transfected with pAcGFP-DGKδ2 (11, 17) using PolyFect (Qiagen) according to the instruction manual and were selected with 800 μg/ml G418 for 2 weeks. Single colonies were isolated and then were then grown in DMEM containing 10% FBS.

RNA Interference—To silence the expression of mouse DGKδ, the following Stealth RNAi duplexes (Invitrogen) were used: DGKδ-siRNA-1, 5′-GAAUGUGAUGCUGGAUCUUACUAAA-3′ and 5′-UUUAGUAAGAUCCAGCAUCACAUUC-3′; DGKδ-siRNA-2, 5′-UGGCAUUGGCUUGGAUGCAAAGAUA-3′ and 5′-UAUCUUUGCAUCCAAGCCAAUGCCA-3′. The duplexes were transfected into C2C12 myoblasts by electroporation (at 350 V and 300 microfarads) using the Gene Pulser Xcell™ electroporation system (Bio-Rad Laboratories). The transfected cells were then allowed to grow for 48 h in DMEM containing 10% FBS.

Glucose Stimulation and Treatment with Lipid Metabolism Enzyme Inhibitors—Glucose stimulation was performed as reported previously (16). Briefly, untransfected C2C12 myoblasts and C2C12 myoblasts transfected with Stealth RNAi duplexes were grown on poly-L-lysine (Sigma-Aldrich)-coated culture dishes. The cells were rinsed and incubated in glucose-free medium (16) in the absence or presence of PC-PLC inhibitor *O*-tricyclo[5.2.1.$0^{2,6}$]dec-9-yl dithiocarbonate (D609, 100 μM, Calbiochem) (22), acetyl-CoA carboxylase inhibitor 5-(tetradecyloxy)-2-furoic acid (TOFA, 20 μM, Calbiochem) (23, 24), or phospholipase D (PLD) inhibitor 5-fluoro-2-indolyl deschlorohalopemide (FIPI, 100 nM, Calbiochem) (25) for 3 h. The cells were incubated for 5 min in the same buffer supplemented with 25 mM glucose.

Lipid Extraction and Western Blot Analysis—The cells grown under each culture condition were harvested and lysed in ice-cold lysis buffer (50 mM HEPES, pH 7.2, 150 mM NaCl, 5 mM $MgCl_2$, 1 mM dithiothreitol, cOmplete™ EDTA-free protease inhibitor (Roche Diagnostics)) followed by centrifugation at 1,000 × *g* for 5 min at 4 °C. Total lipids were extracted from the cell lysates (1.0 mg of protein), in which DGKδ expression was confirmed by Western blot analysis using an anti-DGKδ antibody (13), according to the method of Bligh and Dyer (26). The extracted lipids were used for subsequent MS analyses.

Analysis of PA Molecular Species—PAs in extracted cellular lipids (5 μl) containing 40 pmol of the 14:0/14:0-PA internal standard (Sigma-Aldrich) were analyzed separately by LC/ESI-MS using an Accela LC system (Thermo Fisher Scientific) coupled online to an Exactive Orbitrap MS (Thermo Fisher Scientific) equipped with an ESI source as described previously (21). The MS peaks are presented in the form of *X*:*Y*, where *X* is the total number of carbon atoms and *Y* is the total number of double bonds in both acyl chains of the PA.

For the identification of fatty acid residues in PA molecular species by ESI-MS/MS, PA molecular species (28:0–40:0-PA) were fractionated using the above LC/ESI-MS system equipped with an FC 203B fraction collector (Gilson). The mixture of these isolated PA molecular species was infused into an Exactive Orbitrap MS (Thermo Fisher Scientific) equipped with a syringe pump (an infusion rate of 5 μl/min) and an ESI source. A collision energy of 40 eV was used to obtain fragment ions.

Analysis of DG Molecular Species—The isolation of DG was performed according to previously reported procedures (27). The extracted cellular lipids (per 1 mg of protein) were developed on Silica Gel 60 high performance thin layer chromatography plates (Merck, 10 × 20 cm) using hexane/diethyl ether/acetic acid (75:25:1, v/v). After development, DG was extracted from silica gel and redissolved in 200 μl of methanol:chloroform (9:1, v/v) containing 1 μg/ml 12:0/12:0-DG (Avanti Polar Lipids), and 10 μl of 100 mM sodium acetate were added to each sample (28). MS analysis was performed on an Exactive Orbitrap MS (Thermo Fisher Scientific) equipped with a Fusion 100T syringe pump (an infusion rate of 5 μl/min, Thermo Fisher Scientific) and an ESI source. The ion spray

voltage was set to 5 kV in the positive ion mode. The capillary temperature was set to 300 °C.

Measurement of DGKδ Activity—The octyl glucoside-mixed micellar assay of DGK activity was performed as described previously (12). COS-7 cells transfected with p3×FLAG-DGKδ2 (29) were harvested and lysed in ice-cold lysis buffer followed by centrifugation at 1,000 × *g* for 5 min at 4 °C. The cell lysates were added to octyl glucoside buffer containing 2 mM 16:0/16:0-, 16:0/18:1-, or 18:0/20:4-DG (Avanti Polar Lipids) and 10 mM phosphatidylserine (Avanti Polar Lipids).

Immunoprecipitation and Measurement of PC-PLC Activity—The glucose-stimulated cells stably expressing human DGKδ2 were harvested and lysed in ice-cold lysis buffer (50 mM HEPES, pH7.2, 150 mM NaCl, 5 mM $MgCl_2$, 1% Nonidet P-40, 1 mM dithiothreitol, cOmplete™ EDTA-free protease inhibitor (Roche Diagnostics)) for immunoprecipitation. The mixtures were centrifuged at 12,000 × *g* for 5 min at 4 °C to yield the cell lysates. 500 μg of the cell lysates were incubated with normal rabbit IgG (2 μg, Santa Cruz Biotechnology) or rabbit anti-DGKδ antibody (2 μg) (13, 29) at 4 °C overnight and incubated with protein A/G PLUS-agarose (Santa Cruz Biotechnology) for an additional 1 h. The bead-bound proteins were washed with ice-cold wash buffer (50 mM HEPES, pH 7.2, 100 mM NaCl, 5 mM $MgCl_2$, 0.1% Triton X-100, 10% glycerol, 20 mM NaF) four times and resolved in 70 μl of 1× reaction buffer (50 mM Tris-HCl, pH 7.4, 140 mM NaCl, 10 mM dimethylglutarate, 2 mM $CaCl_2$) in the Amplex Red® PC-PLC assay kit (Molecular Probes-Life Technologies). In this enzyme-coupled assay, PC-PLC activity is monitored indirectly using 10-acetyl-3,7-dihydroxyphenoxazine (Amplex Red® reagent), a sensitive fluorogenic probe for H_2O_2. First, PC-PLC converts PC to form phosphocholine and DG. After the action of alkaline phosphatase, which hydrolyzes phosphocholine, choline is oxidized by choline oxidase to betaine and H_2O_2. Finally, H_2O_2, in the presence of horseradish peroxidase, reacts with Amplex Red® reagent in a 1:1 stoichiometry to generate the highly fluorescent product, resorufin. Resorufin has absorption and fluorescence emission maxima of ~571 nm and 585 nm, respectively. 50-μl aliquots of the mixtures were used for the measurement of PC-PLC activities, and 10 μl of the mixtures were used for Western blot analysis.

Statistics—All LC/ESI-MS data were normalized based on the protein content and the intensity of the internal standard. The data were represented as the mean ± S.D. Statistical analysis was performed using the two-tailed *t* test or analysis of variance followed by Tukey's post hoc test.

RESULTS

Increase in the Amount of PA by Acute Stimulation with High Glucose—We first examined whether the amount of total PA was increased in C2C12 myoblasts stimulated with 25 mM glucose. As shown in Fig. 1*A*, LC/ESI-MS analysis indicated that exposure to high glucose levels (for 5 min) statistically increased the total PA amounts (1.23-fold, $p < 0.005$). In addition, the stimulation significantly increased the amounts of C30 to C36 PA molecular species, with the exception of 36:1-PA (Fig. 1*B*). However, the stimulation did not substantially affect the production of C38 to C40 PA molecular species, including 38:4-PA, with the exception of 38:6-PA.

We investigated the high glucose-dependent increases of total PA amount and PA molecular species in C2C12 myoblasts at different time points. After 5 min of glucose stimulation, the levels of total PA and PA molecular species were significantly increased (Fig. 1, *C* and *D*). However, total PA and PA molecular species levels returned close to basal levels by prolonging the incubation with high glucose concentrations for up to 15 and 30 min. We confirmed that DGK activity *in vitro* was increased by glucose stimulation for 5 min (data not shown). These results strongly suggest that C2C12 myoblasts and L6 myotubes (16) have essentially the same lipid metabolism pathway to produce PA in response to acute glucose stimulation.

We confirmed the changes in the amounts of PA molecular species in C2C12 myotubes in response to acute high glucose stimulation (5 min). The glucose-stimulated C2C12 myotubes showed essentially the same results (Fig. 1, *E* and *F*) as those obtained with C2C12 myoblasts (Fig. 1, *A* and *B*). The results support that C2C12 myoblasts and myotubes possess essentially the same lipid metabolism pathway to produce PA in response to high glucose stimulation. Because C2C12 myoblasts were more efficiently transfected with siRNAs than C2C12 myotubes, C2C12 myoblasts were used for identification of PA molecular species produced by DGKδ in response to high glucose stimulation.

Effects of DGKδ-specific siRNAs on High Glucose-induced Increases in PA Molecular Species—To clarify whether the glucose-stimulated production of PA molecular species is catalyzed by DGKδ, we investigated the effects of a DGKδ-specific siRNA, DGKδ-siRNA-1. Of the two alternatively spliced DGKδ products, DGKδ1 and DGKδ2 (11), C2C12 myoblasts predominantly expressed DGKδ2 (Fig. 2*A*). DGKδ-siRNA-1 efficiently suppressed DGKδ2 expression in C2C12 myoblasts (Fig. 2*A*). To facilitate comparison, averages of the relative values (+glucose *versus* −glucose) from four independent experiments are displayed (Fig. 2*B*). Interestingly, the suppression of DGKδ expression by DGKδ-siRNA-1 significantly inhibited the glucose stimulation-dependent production of saturated fatty acid-containing C30-C34 PA species, 30:0-, 32:0-, and 34:0-PA, to their basal levels. In addition, one saturated and one monounsaturated fatty acid-containing PA, 34:1-PA, decreased as well. However, the amount of arachidonic acid (20:4)-containing PA, 38:4-PA, was not markedly changed (Fig. 2*B*). To rule out off-target effects of DGKδ-siRNA-1, we employed an independent siRNA targeted to a different region of DGKδ mRNA (DGKδ-siRNA-2). DGKδ-siRNA-2, which suppressed DGKδ2 expression slightly less strongly than DGKδ-siRNA-1 (Fig. 2*C*), also statistically inhibited the production of 30:0-, 34:1-, and 34:0-PA and moderately attenuated 32:0-PA generation (Fig. 2*D*). These results suggest that DGKδ selectively phosphorylated 30:0-, 32:0-, 34:1-, and 34:0-DG, which contain either two saturated fatty acids or one saturated and one monounsaturated fatty acids, but not 38:4-PA.

We investigated whether the decreases in the amounts of 30:0-, 32:0-, 34:1-, and 34:0-PA by DGKδ-siRNAs were due to decreases in the substrates, the corresponding DG species, in high glucose-stimulated and -unstimulated C2C12 myoblasts.

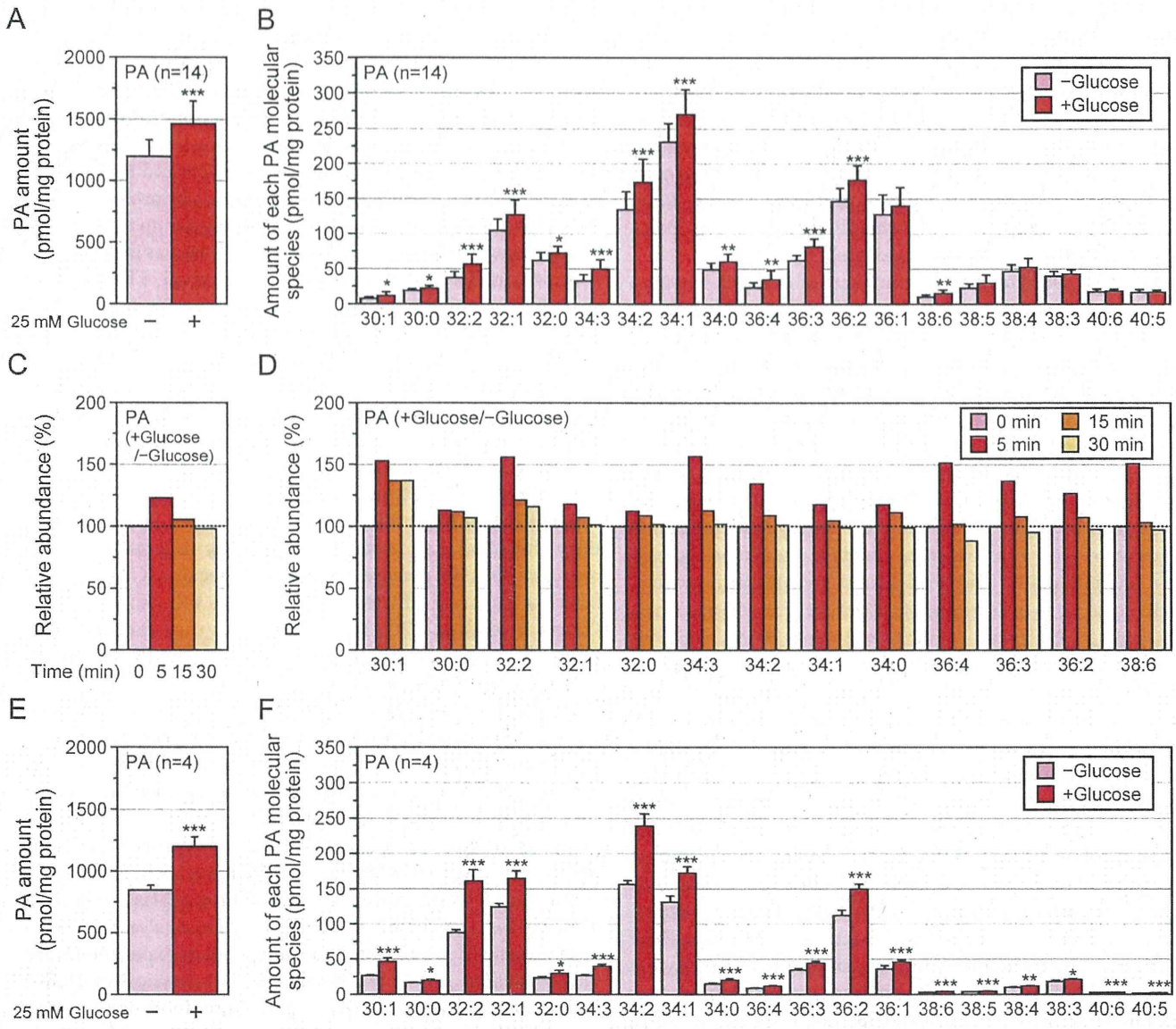

FIGURE 1. **Changes in the total PA and PA molecular species by high glucose stimulation in C2C12 myoblasts and myotubes.** *A* and *B*, the amounts of the total PAs (*A*) and major PA molecular species (*B*) in the glucose-unstimulated or glucose-stimulated C2C12 myoblasts were quantified using the LC/ESI-MS method. The values are presented as the mean ± S.D. ($n = 14$). *, $p < 0.05$; **, $p < 0.01$; ***, $p < 0.005$ (no stimulation *versus* glucose stimulation). *C* and *D*, the amounts of the total PAs (*C*) and major PA molecular species (*D*) that statistically increased in *A* in the cells stimulated by glucose for 5, 15, or 30 min were detected using the LC/ESI-MS method. The results are presented as the percentage of the value of PA molecular species in glucose-unstimulated cells. The values are presented as the mean ($n = 2$). Essentially the same results were obtained in two independent experiments. *E* and *F*, the amounts of the total PAs (*E*) and major PA molecular species (*F*) in the glucose-unstimulated or glucose-stimulated C2C12 myotubes were quantified using the LC/ESI-MS method. The values are presented as the mean ± S.D. ($n = 4$). *, $p < 0.05$; **, $p < 0.01$; ***, $p < 0.005$ (no stimulation *versus* glucose stimulation).

Glucose stimulation substantially increased the amounts of various DG species (Fig. 3). However, DGKδ-siRNA-1 failed to significantly affect the amounts of 30:0-, 32:0-, 34:1-, and 34:0-DG molecular species both in the absence and in the presence of high glucose levels. Therefore, it is likely that the decreases in the amounts of 30:0-, 32:0-, 34:1-, and 34:0-PA were not caused by decreased amounts of the corresponding DG species.

Effect of Overexpression of DGKδ on the Production of PA Molecular Species—To confirm the results of the siRNA experiments, we evaluated the result of DGKδ2 overexpression on high glucose-dependent production of PA species in C2C12 cells. In response to high glucose, the levels of 30:0-, 32:0-, and 34:0-PA statistically increased in C2C12 cells stably expressing DGKδ2 when compared with control cells (Fig. 4*B*). Moreover, 30:1- and 32:1-PA were also augmented. In contrast, 38:4-PA did not increase. Taken together with the siRNA results (Figs. 2 and 4), these results support the hypothesis that DGKδ phosphorylated DG species with an apparent preference for 30:0-, 32:0-, and 34:0-DG, but not arachidonic acid-containing DG, 38:4-DG. Moreover, it is possible that this enzyme also generates 30:1-, 32:1-, and 34:1-PA.

Fatty Acid Composition of 30:0-, 32:0-, and 34:0-PA—We next determined the molecular identities of the two fatty acids included in 30:0-, 32:0-, and 34:0-PA, which were indicated to be selectively generated by DGKδ2 in C2C12 cells. ESI-MS/MS

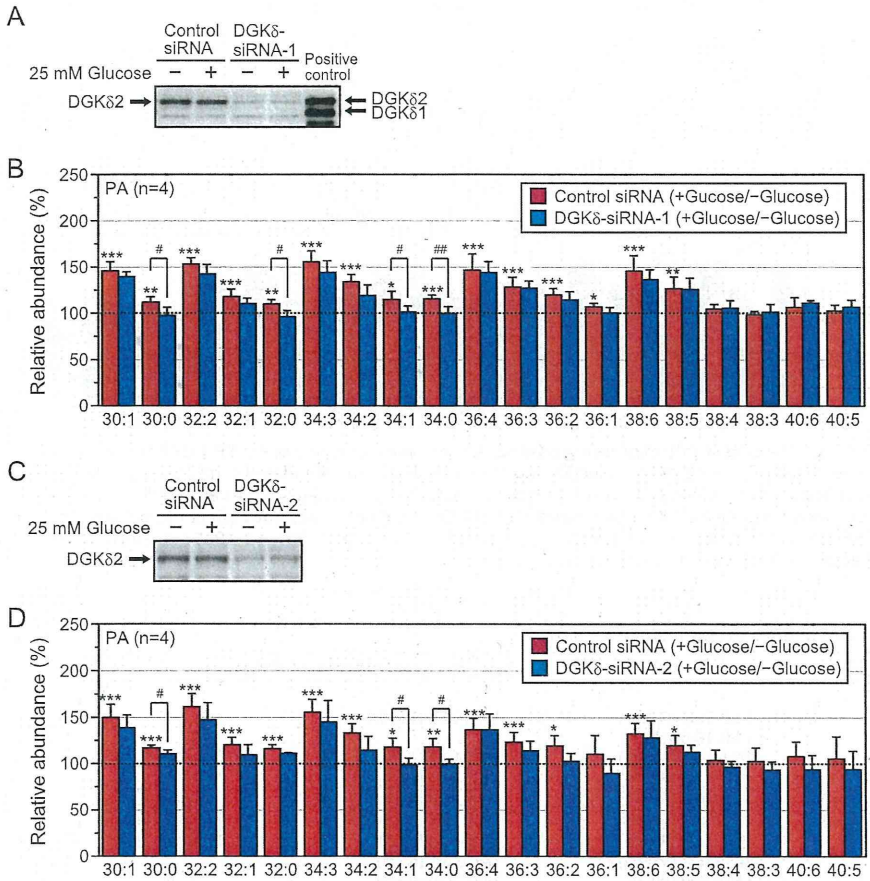

FIGURE 2. **Effects of DGKδ-siRNA-1 and -2 on high glucose-induced increases of PA molecular species in C2C12 myoblasts.** *A* and *C*, the suppression of DGKδ2 expression by DGKδ-siRNA-1 (*A*) or DGKδ-siRNA-2 (*C*) was confirmed by Western blot analysis using the anti-DGKδ antibody. Human DGKδ1 and DGKδ2 (11) expressed in COS-7 cells were electrophoresed as a control (*A*). *B* and *D*, the major PA molecular species in the glucose-unstimulated or glucose-stimulated cells transfected with control siRNA or DGKδ-siRNA-1/2 were detected using the LC/ESI-MS method. The results are presented as the percentage of the value of PA molecular species in glucose-unstimulated cells transfected with control siRNA or DGKδ-siRNA-1/2. DGKδ-siRNA-1/2 did not significantly affect the value of PA molecular species in glucose-unstimulated cells. The values are presented as the mean ± S.D. ($n = 4$). *, $p < 0.05$; **, $p < 0.01$; ***, $p < 0.005$ (no stimulation *versus* glucose stimulation). #, $p < 0.05$; ##, $p < 0.01$ (control siRNA *versus* DGKδ-siRNA-1 or DGKδ-siRNA-2).

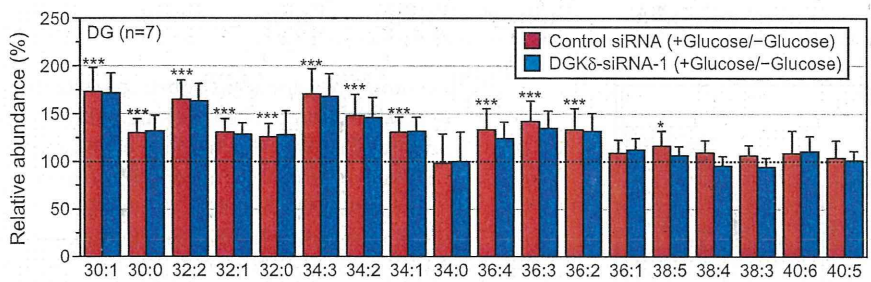

FIGURE 3. **Effect of DGKδ-siRNA-1 on high glucose-induced increases of DG molecular species in C2C12 myoblasts.** The major DG molecular species in the glucose-unstimulated or glucose-stimulated cells transfected with control siRNA or DGKδ-siRNA-1 were detected using the ESI-MS method. The results are presented as the percentage of the value of DG molecular species in glucose-unstimulated cells transfected with control siRNA or DGKδ-siRNA-1. DGKδ-siRNA-1 did not significantly affect the value of DG molecular species in glucose-unstimulated cells. The values are presented as the mean ± S.D. ($n = 7$). *, $p < 0.05$; ***, $p < 0.005$ (no stimulation *versus* glucose stimulation).

analysis revealed that the main fatty acid residues were as follows: 30:0 consisted of 14:0 and 16:0 (100%), 32:0 included 16:0 and 16:0 (96.6%), and 34:0 contained 16:0 and 18:0 (99.7%) (Table 1). These results indicate that 30:0-, 32:0-, and 34:0-PA consist of relatively short saturated fatty acids and commonly contain palmitic acid (16:0). It is possible that DGKδ2 also produces 30:1-, 32:1-, and 34:1-PA species (Figs. 2 and 4). These PA species contain saturated fatty acids, 16:0 and 14:0, and monounsaturated fatty acids, 16:1 and 18:1 (Table 1).

In Vitro DGKδ Activity—We examined whether the preference of DGKδ2 for palmitic acid (16:0)-containing DG species, 30:0-, 32:0-, and 34:0-DG, is an intrinsic catalytic feature of DGKδ. To this end, we measured DGKδ2 activity *in vitro* using 32:0 (16:0/16:0)-, 34:1 (16:0/18:1)-, or 38:4 (18:0/20:4)-DG as

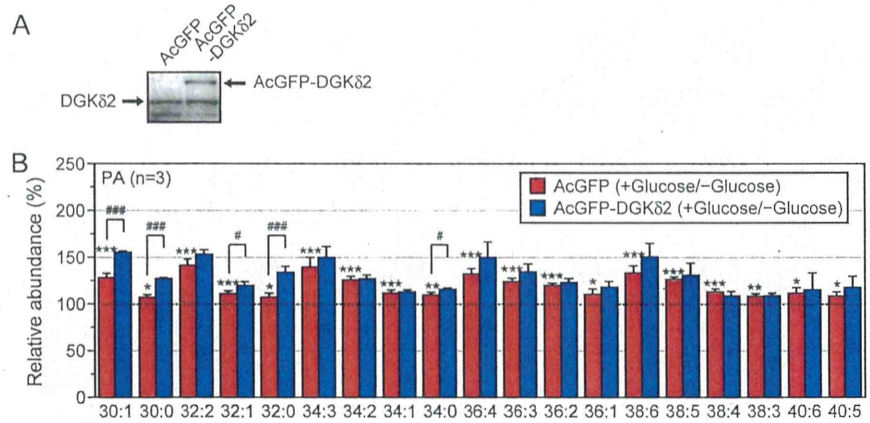

FIGURE 4. **PA molecular species in C2C12 cells stably expressing DGKδ2.** *A*, the stable expression of AcGFP-DGKδ2 in C2C12 cells was confirmed by Western blot analysis using the anti-DGKδ antibody. *B*, the major PA molecular species in the glucose-unstimulated or glucose-stimulated cells stably expressing human DGKδ2 were identified and quantified using LC/ESI-MS. The results are presented as the percentage of the value of PA molecular species in glucose-unstimulated cells transfected with AcGFP alone or AcGFP-DGKδ2. Overexpression of DGKδ2 did not significantly affect the value of PA molecular species in glucose-unstimulated cells. The values are presented as the mean ± S.D. ($n = 3$). *, $p < 0.05$; **, $p < 0.01$; ***, $p < 0.005$ (no stimulation *versus* glucose stimulation). #, $p < 0.05$; ###, $p < 0.005$ (no overexpression *versus* DGKδ overexpression).

TABLE 1
Identification of the acyl species in each PA molecular species

PA molecular species	Identified acyl chains[a]			
	%			
30:1	14:0/16:1 (86.0%)	16:0/14:1 (14.0%)		
30:0	14:0/16:0 (100%)			
32:2	16:1/16:1 (98.5%)	14:0/18:2 (1.5%)		
32:1	16:0/16:1 (88.7%)	14:0/18:1 (11.3%)		
32:0	16:0/16:0 (96.6%)	14:0/18:0 (3.4%)		
34:3	16:1/18:2 (67.2%)	16:2/18:1 (27.7%)	16:0/18:3 (5.1%)	
34:2	16:1/18:1 (86.3%)	16:0/18:2 (13.6%)	16:2/18:0 (0.1%)	
34:1	16:0/18:1 (93.2%)	18:0/16:1 (6.8%)		
34:0	16:0/18:0 (99.7%)	14:0/20:0 (0.3%)		
36:4	16:0/20:4 (83.0%)	16:1/20:3 (8.7%)	18:1/18:3 (7.2%)	18:2/18:2 (1.2%)
36:3	18:1/18:2 (74.9%)	16:0/20:3 (23.6%)	16:1/20:2 (0.8%)	18:0/18:3 (0.7%)
36:2	18:1/18:1 (91.6%)	18:0/18:2 (5.0%)	16:0/20:2 (2.5%)	16:1/20:1 (0.9%)
36:1	18:0/18:1 (87.8%)	16:0/20:1 (6.5%)	16:1/20:0 (5.6%)	14:0/22:1 (0.1%)
38:6	16:0/22:6 (68.0%)	16:1/22:5 (30.9%)	18:1/20:5 (1.1%)	
38:5	16:0/22:5 (45.0%)	18:1/20:4 (45.0%)	18:0/20:5 (8.5%)	16:1/22:4 (1.6%)
38:4	18:0/20:4 (80.1%)	18:1/20:3 (19.5%)	16:0/22:4 (0.4%)	
38:3	18:0/20:3 (88.6%)	18:1/20:2 (10.5%)	16:0/22:3 (0.9%)	
40:6	18:1/22:5 (51.5%)	18:0/22:6 (47.6%)	16:0/24:6 (0.9%)	
40:5	18:0/22:5 (97.4%)	18:1/22:4 (2.6%)		

[a] The relative abundance (%) was based on the peak areas of the fragment ions (ESI-MS/MS) for each molecular ion.

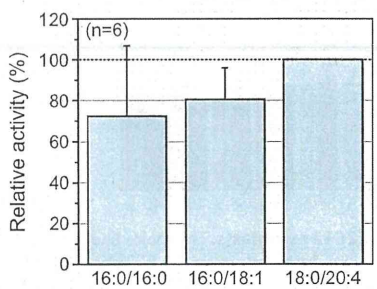

FIGURE 5. ***In vitro* DGKδ activity.** For measurement of *in vitro* DGKδ activity, 2 mM (5.4 mol%) 16:0/16:0-, 16:0/18:1-, and 18:0/20:4-DG were used as substrates. The activity of 3×FLAG-tagged DGKδ2 in COS-7 cells was compared with the control. The results are presented as the percentage of the value of activity against 18:0/20:4-DG. The values are presented as the mean ± S.D. ($n = 6$).

substrates. As shown in Fig. 5, the levels of 32:0- and 34:1-PA generated by DGKδ2 were similar to or slightly lower than that of 38:4-PA. These results indicate that DGKδ2 does not exhibit intrinsic substrate selectivity for particular DG molecular species, 32:0-DG, *in vitro*. Therefore, we hypothesized that DGKδ accomplishes apparent substrate selectivity in C2C12 cells by accessing a DG pool containing only 30:0-, 32:0-, and 34:0-DG, and not based on the intrinsic properties of the enzyme.

Effects of Inhibitors of Lipid Metabolism Enzymes on High Glucose Level-induced PA Production—To test this hypothesis, we next searched for the lipid metabolic pathway that supplies 30:0-, 32:0-, and 34:0-DG species as a substrate for DGKδ2. There are three pathways that produce DG, 1) the *de novo* pathway (30, 31), 2) the PLD/PA phosphatase pathway (32), and 3) the PC-specific PLC pathway (33). The treatment with 20 μM TOFA, which inhibits acetyl-CoA carboxylase involved in the *de novo* synthesis of DG (23, 24), did not decrease the glucose-stimulated production of PA molecular species (Fig. 6*A*). Moreover, 100 nM FIPI, which inhibits PLD involved in DG generation from PC through the action of PA phosphatase (25), reduced the amounts of most of the PAs in the absence of high glucose stimulation (data not shown). However, this compound failed to attenuate the glucose-stimulated production of PA molecular species (Fig. 6*B*). These results strongly suggest that these pathways are not involved in the DG supply to DGKδ2.

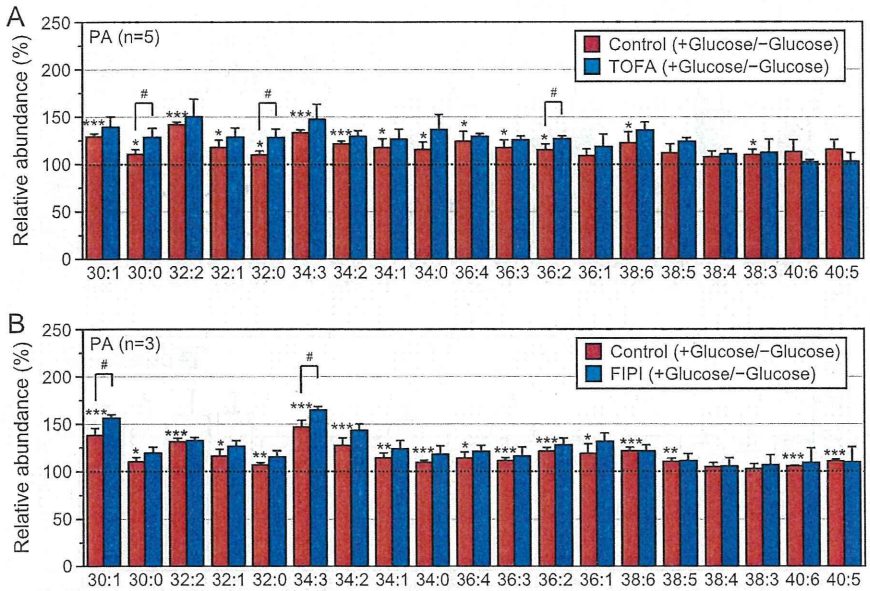

FIGURE 6. **Effects of TOFA and FIPI on the production of PA molecular species in glucose-stimulated C2C12 cells.** *A*, the major PA molecular species in glucose-unstimulated or glucose-stimulated cells treated with DMSO (control) or TOFA were detected using the LC/ESI-MS method. The results are presented as the percentage of the value of PA species in glucose-unstimulated cells treated with DMSO (control) or TOFA. The values are presented as the mean ± S.D. ($n = 5$). *, $p < 0.05$; ***, $p < 0.005$ (no stimulation *versus* glucose stimulation). #, $p < 0.05$ (without TOFA *versus* with TOFA). *B*, the major PA molecular species in the glucose-unstimulated or glucose-stimulated cells treated with DMSO (control) or FIPI were detected using the LC/ESI-MS method. The results are presented as the percentage of the value of PA species in glucose-unstimulated cells treated with DMSO (control) or FIPI. The values are presented as the mean ± S.D. ($n = 3$). *, $p < 0.05$; **, $p < 0.01$; ***, $p < 0.005$ (no stimulation *versus* glucose stimulation). #, $p < 0.05$ (without FIPI *versus* with FIPI).

D609 is an inhibitor of PC-PLC (22), which generates DG via PC hydrolysis (34). Treatment with 100 μM D609 strongly inhibited the high glucose stimulation-responsive production of 30:0-, 32:0-, and 34:0-PA to their basal levels (Fig. 7*A*), suggesting that DGKδ2 utilizes DG species supplied from the PC-PLC pathway.

We next confirmed that D609 inhibited the production of DG molecular species, including 30:0-, 32:0-, and 34:0-DG. This inhibitor statistically attenuated the amounts of 30:0-, 32:0-, and 34:0-DG in the absence of high glucose stimulation (Fig. 7*B*). However, D609 inhibited high glucose-dependent increases for all of the C30-C34 DG species (Fig. 7*C*). These results suggest that, in response to acute high glucose stimulation (5 min), DGKδ2 can utilize DG species that are supplied from the PC-PLC pathway, in both high glucose-independent and high glucose-dependent manners.

Linkage between PC-PLC and DGKδ—To further examine the linkage between the PC-PLC pathway and DGKδ2, we determined whether D609 and DGKδ-siRNA-1 additively affected the high glucose-dependent increases of 30:0-, 32:0-, and 34:0-PA. If DGKδ2 utilizes DG species supplied from the PC-PLC pathway, it would be expected that reduced expression of DGKδ2 via DGKδ-siRNA-1 would not enhance the effect of the PC-PLC inhibitor. It was confirmed that the expression of DGKδ2 was substantially reduced by DGKδ-siRNA-1, even in the presence of D609 (Fig. 8*A*). As shown in Fig. 8*B*, DGKδ-siRNA-1 failed to further inhibit the glucose-dependent increases of 30:0-, 32:0-, and 34:0-PA in the presence of D609. These results strongly suggest that 30:0-, 32:0-, and 34:0-DG phosphorylated by DGKδ2 in response to acute high glucose exposure are generated, at least in part, by PC hydrolysis catalyzed by PC-PLC.

We next examined whether DGKδ directly or indirectly interacted with PC-PLC. To this end, we used C2C12 cells stably overexpressing DGKδ2 (Fig. 4) and stimulated the cells with high glucose. We confirmed that DGKδ2 was immunoprecipitated with the anti-DGKδ antibody (Fig. 8*C*). Because the molecular identity of mammalian PC-PLC remains unclear (35), its antibody is unavailable. Therefore, we determined PC-PLC activity in the immunoprecipitates using the Amplex Red® PC-PLC assay kit, which detects phosphocholine generated by PC-PLC. As demonstrated in Fig. 8*D*, PC-PLC activity was clearly co-immunoprecipitated with DGKδ2. The assay does not detect the activity of sphingomyelin synthase, which produces DG and sphingomyelin, but not phosphocholine. The contribution of PLD, which hydrolyzes PC to PA and choline, can be accounted for by elimination of alkaline phosphatase from the assay (see "Experimental Procedures"). However, when the assay was performed in the absence of alkaline phosphatase, the activity was not detectable. Taken together, these results strongly suggest that DGKδ2 utilizes DG species supplied from PC-PLC-dependent PC hydrolysis in response to high glucose (Fig. 9).

DISCUSSION

The increase in PA molecular species by stimulation with high glucose levels has not been identified until now. Moreover, it has not been reported that high glucose induces total PA production. The main reasons for this are that PA species are minor components and it is difficult to quantify the amounts of PA molecular species using conventional LC/ESI-MS methods. To overcome this difficulty, we recently established an LC/ESI-MS method specialized for PA species (21). In this study, we revealed for the first time that acute high glucose